Cyclopentadienyl ligands in lanthanide single-molecule magnets: One ring to rule them all?

Benjamin M Day, Fu-Sheng Guo, Richard Layfield

Publication date
09-06-2023

Document Version
Accepted version

Citation for this work (American Psychological Association 7th edition)
Day, B. M., Guo, F.-S., & Layfield, R. (2018). *Cyclopentadienyl ligands in lanthanide single-molecule magnets: One ring to rule them all?* (Version 1). University of Sussex. https://hdl.handle.net/10779/uos.23460899.v1

Published in
Accounts of Chemical Research

Link to external publisher version
https://doi.org/10.1021/acs.accounts.8b00270

Cyclopentadienyl Ligands in Lanthanide Single-Molecule Magnets: One Ring to Rule Them All?

Benjamin M. Day,[1] Fu-Sheng Guo,[1] Richard A. Layfield[2]*

[1] School of Chemistry, The University of Manchester, Oxford Road, Manchester, M13 9PL, U.K.

[2] Department of Chemistry, School of Life Sciences, University of Sussex, Brighton, BN1 9QJ

R.Layfield@sussex.ac.uk

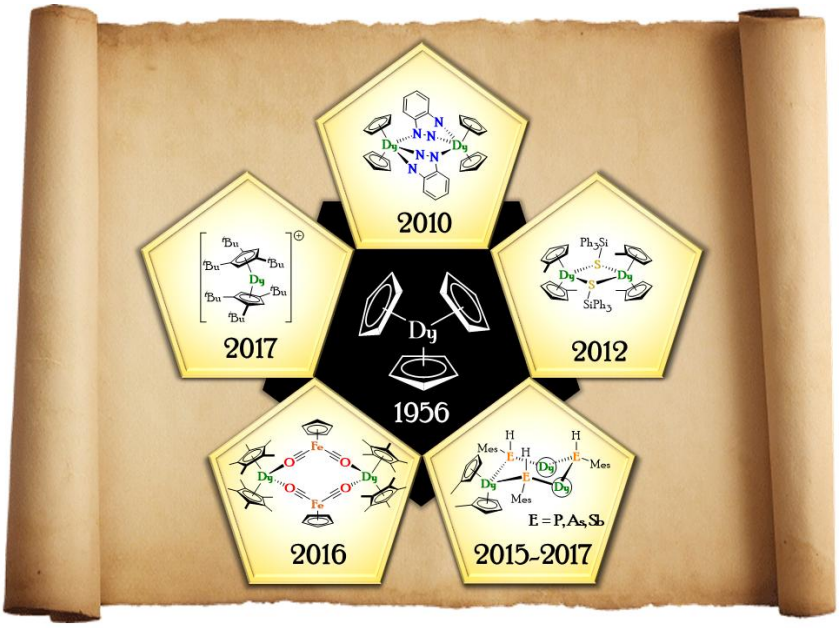

CONSPECTUS

The discovery of materials capable of storing magnetic information at the level of single molecules and even single atoms has fueled renewed interest in the slow magnetic relaxation properties of single-molecule magnets (SMMs). The lanthanide elements – especially dysprosium – continue to play a pivotal role in the development of potential nanoscale applications of SMMs, including, for example, in molecular spintronics and quantum computing. Aside from their fundamentally fascinating physics, the realization of functional materials based on SMMs requires significant scientific and technical challenges to be overcome. In particular, extremely low temperatures are needed to observe slow magnetic relaxation, and whilst many SMMs possess a measurable energy barrier to reversal of the magnetization (U_{eff}), very few such materials display the important properties of magnetic hysteresis with remanence and coercivity.

Werner-type coordination chemistry has been the dominant method used in the synthesis of lanthanide SMMs, and most of our knowledge and understanding of these materials is built on the many important contributions based on this approach. In contrast, lanthanide organometallic chemistry and lanthanide magnetochemistry have effectively evolved along separate lines, hence our goal was to promote a new direction in single-molecule magnetism by uniting the non-classical organometallic synthetic approach with the traditionally distinct field of molecular magnetism. Over the last several years, our work on SMMs has focused on obtaining a detailed understanding of why magnetic materials based on the dysprosium metallocene cation building block $\{Cp_2Dy\}^+$ display slow magnetic relaxation. Specifically, we aspired to control the SMM properties using novel coordination chemistry in a way that hinges on key considerations, such as the strength and the symmetry of the crystal field. In establishing that the two cyclopentadienyl ligands combine to provide a strongly axial crystal field, we were able to

propose a robust magneto-structural correlation for understanding the properties of dysprosium metallocene SMMs. In doing so, a blueprint was established that allows U_{eff} and the magnetic blocking temperature (T_B) to be improved in a well-defined way.

Although experimental discoveries with SMMs occur more rapidly than quantitative theory can (currently) process and explain, a clear message emanating from the literature is that a combination of the two approaches is most effective. In this Account, we summarize the main findings from our own work on dysprosium metallocene SMMs, and consider them in the light of related experimental studies and theoretical interpretations of related materials reported by other protagonists. In doing so, we aim to contribute to the nascent and healthy debate on the nature of spin dynamics in SMMs and allied molecular nanomagnets, which will be crucial for the further advancement of this vibrant research field.

1. INTRODUCTION

Organometallic chemistry has accounted for many significant advances in our understanding of the lanthanides, with η^n-bonded carbocyclic ligands playing a central role in developing the field.[1] Since the bonding in lanthanide compounds is predominantly electrostatic, their organometallic chemistry is dominated by anionic ligands, but none more so than cyclopentadienyl (Cp) ligands. Following the pioneering work of Birmingham and Wilkinson on the first lanthanide cyclopentadienyls,[2] careful applications of the textbook principles of lanthanide chemistry have enabled striking progress. For example, the facile σ-bond metathesis reaction of methane with the simple metallocene [Cp*$_2$LuMe] provided the first example of methane activation by a homogeneous organometallic complex.[3] Catalytic applications of lanthanide cyclopentadienyl compounds continue to be developed, often resulting in unique reactivity owing to the distinctive molecular and electronic structures of the metals.[4] Given that lanthanides tend to be stuck in the +3 oxidation state, their compounds are not an obvious choice as reducing agents. However, the bulky cyclopentadienyl complexes [Cp*$_3$M] show a remarkable ability to transfer electrons to various substrates through ligand-based oxidations, reactivity known as sterically induced reduction.[5] Following Lappert's discovery of the first non-traditional divalent rare-earth complex, i.e. the lanthanum(II) species [La{1,3-(Me$_3$Si)$_2$C$_5$H$_3$}$_3$]$^-$,[6] cyclopentadienyl ligands have provided a route into the divalent oxidation state for all lanthanides (except radioactive promethium) in the series [M{(Me$_3$Si)C$_5$H$_4$}$_3$]$^-$.[7,8] The determination of $4f^n$ $5d^1$ ground-states for some of these complexes and $4f^{n+1}$ for others revealed, for the first time, the ligand-dependent electronic structure of divalent lanthanides.[8]

One aspect of lanthanide organometallic chemistry that remains underdeveloped is magnetism. The main reason for the paucity of detailed studies on the magnetic properties of lanthanide organometallics is readily understood: crystal field effects are assumed to be insignificant, the free-ion approximation holds under normal synthetic conditions and, hence, the magnetic properties have no bearing on reactivity. Whilst this approach is adequate from a practical perspective, it neglects the intrinsically fascinating electronic structure of lanthanides, particularly at low temperatures, where the properties of the crystal field become critical considerations in explaining the properties. Strictly speaking, the magnetochemistry of lanthanide organometallics is nothing more than a specialized focus on a certain class of ligand within the wider family of lanthanide coordination compounds. Indeed, the magnetic properties of 'classical' lanthanide coordination compounds have been studied in considerable detail; the main features are well established and readily applicable to their organometallic cousins.[9]

One of the most exciting recent discoveries in lanthanide magnetochemistry is single-molecule magnetism, a phenomenon in which coordination compounds show slow relaxation of the magnetization in a manner that does not rely on cooperative interactions across magnetic domains.[10] Rather, SMM behavior can be assigned to the properties of individual molecules. Following the early advances made with polymetallic manganese single-molecule magnets (SMMs),[11] a step-change occurred with Ishikawa's elegant work on D_{4d}-symmetric terbium and dysprosium phthalocyanine (Pc) sandwiches, which were found to display SMM behavior even though the $[LnPc_2]^{n-}$ complexes (n = 0, 1) only contain a single magnetic center.[12] Subsequently, a huge number of mono- and poly-metallic lanthanide SMMs were reported, with most containing dysprosium.[13] The considerable attention directed towards SMMs initially stemmed from their proposed applications in magnetic information storage.[14] More recently, SMMs have

been used as components in molecular spintronic devices.[15] Of the many challenges to developing functional SMM materials, arguably the most significant is the fact that extremely low temperatures are required to eliminate the processes that result in rapid relaxation of the magnetization. Progress towards overcoming this challenge is typically expressed through two parameters. Firstly, the effective energy barrier to reversal of the magnetization (U_{eff}) is essentially the energy required to flip a magnetic dipole from 'up' to 'down', and is conventionally extracted from measurements of the frequency-dependence of the imaginary component of the A.C. magnetic susceptibility, i.e. $\chi''(\nu)$.[16] The second and, arguably, more important parameter is the magnetic blocking temperature, T_B, which has defied attempts at a strict definition and is variously expressed as: (1) the maximum temperature at which isothermal magnetization *vs*. field hysteresis loops remain open; (2) the temperature at which the relaxation time is 100 seconds, and; (3) the temperature at which the field-cooled and zero-field-cooled molar magnetic susceptibilities (χ_M) diverge. Methods 1 and 3 incorporate time (sweep rate) as a third variable, such that T_B is operator-dependent, and values expressed through these routes should be evaluated in light of the experimental conditions.

Of particular significance for our research was Murugesu's phenolate-bridged SMM $[Dy(hmi)(NO_3)(MeOH)]_2$, where H_2hmi is (2-hydroxy-3-methoxyphenyl)methylene-isonicotino(hydrazine).[17] The Dy_2O_2 core of this SMM is reminiscent of the extensive series of dimeric, heteroatom-bridged lanthanide cyclopentadienyl compounds $[Cp_2Ln(\mu\text{-}X)]_2$, a structural motif known for all lanthanides with many different Cp ligands and bridging ligands.[18] An advantage of organometallic chemistry is that the bridging ligand can be varied across a much broader range of p-block donor atoms than can be achieved with classical coordination chemistry, which allows variations in the crystal field and the exchange interactions to be

explored periodically. The magnetic properties of these cyclopentadienyl compounds have been studied in very few cases.[19] In 2010, it occurred to us that it might be possible to observe SMM behavior in molecules based on the dysprosium metallocene $\{Cp_2Dy\}^+$ unit, and so began our program of research in this area.

2. SYNTHESIS AND STRUCTURE OF DYSPROSIUM METALLOCENE SMMs

2.1. Why dysprosium?

The physics of lanthanide SMMs have been the subject of many excellent reviews and monographs,[9,20] and only the essential features will be covered here. Firstly, the spin-orbit coupled ground state of the $4f^9$ ion Dy^{3+} is represented by the $^6H_{15/2}$ term symbol, which reflects a very strong orbital contribution to the magnetic moment. Secondly, the critical property to consider when designing an SMM is magnetic anisotropy, and Dy^{3+} is almost unrivalled owing to the strongly oblate spheroidal shape of its electron density. The anisotropy of dysprosium is therefore enhanced in environments that generate a strong axial crystal field (i.e. perpendicular to the plane of the long spheroidal axes) and a weak equatorial crystal field (i.e. coplanar with the long spheroidal axes).[21] This simple yet crucial design principle can be extended in a complementary manner to erbium(III), which possesses prolate electron density that allows SMM behavior to be observed in systems with strong equatorial crystal fields, such as $[Er(\eta^8\text{-}COT)_2]^-$ and related SMMs.[22] Thirdly, because Dy^{3+} is described by Kramers' theorem, which states that the energy levels of any system with an odd number of electrons must be at least doubly degenerate in an electric field,[23] the coordination environment does not need to be perfectly axial for the molecule to show magnetic bi-stability, i.e. SMM behavior.

Thus, making an SMM is easy: just add dysprosium. However, making a 'good' SMM requires more careful thought, and understanding a particular SMM in a way that leads to targeted improvements in the properties, represents real progress. In the following sections, we show how our initial approach was rewarded with good fortune, which subsequently led to the development of a magneto-structural correlation that allows the SMM properties of dysprosium metallocenes to be enhanced in a rational way.

2.2. Synthesis of Dysprosium Metallocene SMMs

A consideration of the ionic bonding in lanthanide cyclopentadienyl compounds allowed us to develop general methods for the targeted synthesis of structurally similar SMMs with different bridging ligands (Chart 1). The simplest route involved direct deprotonation of acidic E–H substrates by $(Cp^R)_3Dy$ (E = p-block element; $Cp^R = C_5H_5$ or C_5H_4Me), which gave the nitrogen-bridged dimer $[Cp_2Dy(\mu\text{-bta})]_2$ (**1**, bta = benzotriazolate)[24] and the selenolate-bridged trimer $[(\eta^5\text{-}Cp'_2Dy)\{\mu\text{-}SeMes\}]_3$ (**2**, Mes = mesityl).[25] For weakly acidic pro-ligands, lithiation of the pro-ligand followed by reaction with $(Cp^{Me})_3Dy$ and elimination of $Cp^{Me}Li$ is an effective route to the thiolate-bridged dimer $[(Cp^{Me})_2Dy(\mu\text{-}SSiPh_3)]_2$ (**3**).[26] Combinations of $(Cp^{Me})_3Dy$ and $MesEH_2$ (E = P, As) give the Lewis adducts $[(Cp^{Me})_3DyE(H)_2Mes]$, which can be deprotonated by ^{n}BuLi to give the phosphide- and arsenide-bridged trimers $[(\eta^5\text{-}Cp'_2Dy)\{\mu\text{-}ER(H)Mes\}]_3$ (**4P**, **4As**).[25,27] Further deprotonation of **4P** and **4As** by ^{n}BuLi produced the phosphinidene- and arsinidene-bridged species $[Li(thf)_4]_2[(\eta^5\text{-}Cp'_2Dy)_3(\mu_3\text{-}EMes)_3Li]$ (**5P** and **5As**), the latter being the first lanthanide arsinidene complex.[28] The use of more reactive $[(Cp^{Me})_2Dy(^n Bu)]_2$ (**6**)

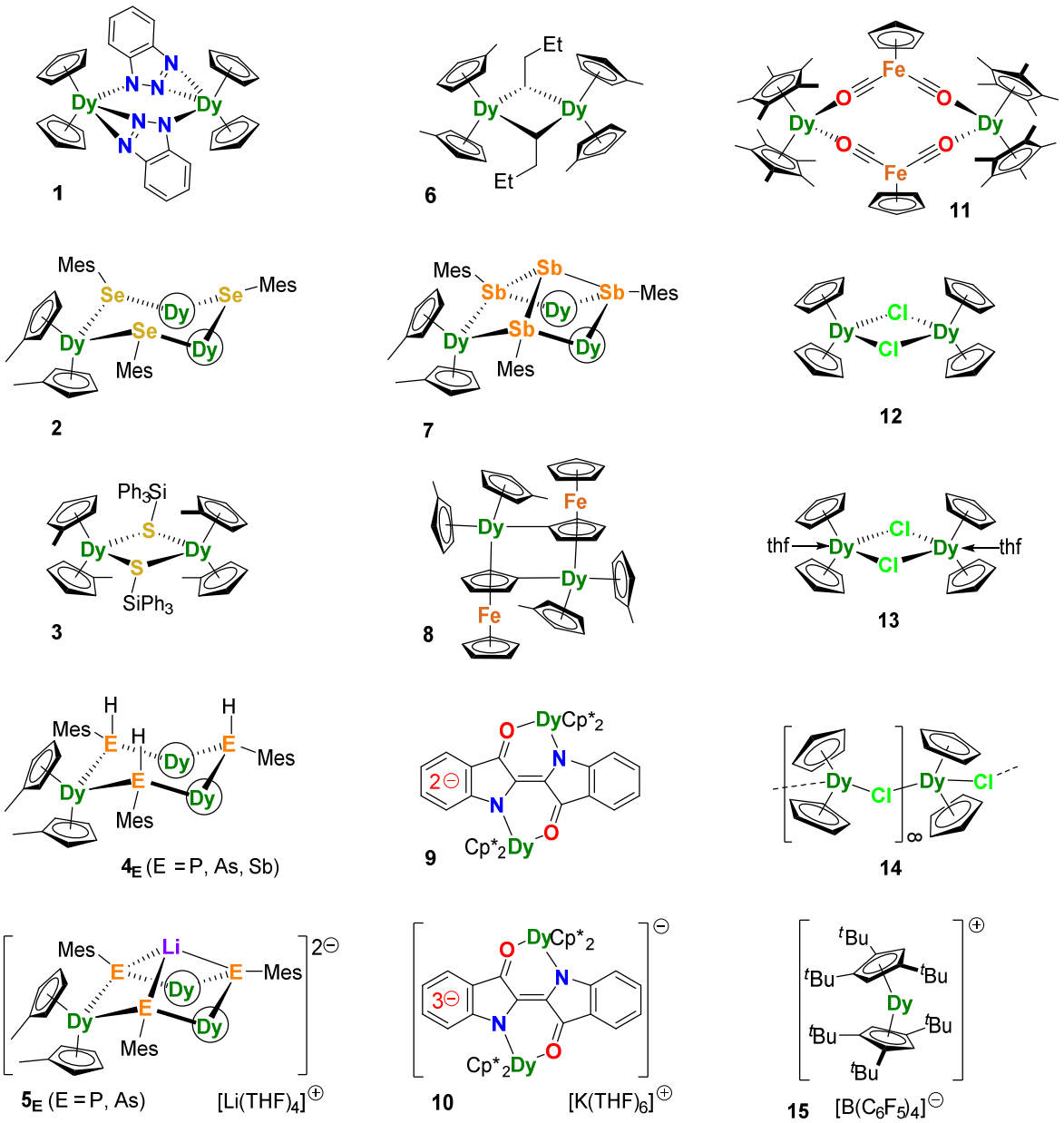

Chart 1. Dysprosium metallocene SMMs.

allowed deprotonation of $MesSbH_2$ to give the stibinide complex $[(\eta^5\text{-}Cp'_2Dy)\{\mu\text{-}ER(H)Mes\}]_3$ ($\mathbf{4_{Sb}}$).[29] Although the stibinidene analogue of $\mathbf{4_{Sb}}$ could not be isolated, it was possible to convert

this compound into the unusual Zintl-bridged complex **7** through a dehydrocoupling reaction with $MesSbH_2$.

Compound **6** also deprotonates ferrocene to give the double sandwich compound $[(Cp^{Me})_2Dy(\kappa{:}\eta^5\text{-}C_5H_4)FeCp]_2$ (**8**).[30] Deprotonation of indigo by $[Cp^*_2Dy(\eta^3\text{-}C_3H_5)]$ allowed isolation of $[(Cp^*_2Ln)_2(\mu\text{-ind})]$ (**9**), and reduction of **9** by KC_8 gave the radical-bridged salt $[K(thf)_6][(Cp^*_2Ln)_2(\mu\text{-ind})]$ ($[K(thf)_6][\mathbf{10}]$).[31] Finally, salt metathesis provided access to the isocarbonyl-bridged metallocene $[Cp^*_2Dy(\mu\text{-Fp})]_2$ (**11**, Fp = $CpFe(CO)_2$) from KFp and $[Cp^*_2Dy(BPh_4)]$,[32] and to the chloride-bridged compounds $[Cp_2Dy(\mu\text{-Cl})]_n$ (n = 2, **12**; $n = \infty$, **13**) and $[Cp_2Dy(\mu\text{-Cl})(thf)]_2$ (**14**).[33]

Our synthetic approach yielded a broad range of metallocene SMMs, and our next aim was to understand how different hard and soft donor atoms influence the magnetism of $[Cp_2Dy]^+$ units and the exchange interactions between them. The broader significance of the pnictogen-ligated SMMs **4** and **5** stems from the fact that heavier p-block elements are very rarely studied in molecular magnetism. In focusing on heavier p-block ligands, we sought to explore the impact of variations in the covalency on the properties, and whether or not the spin-orbit coupling properties of the donor atoms influence the magnetism in a meaningful way.

3. MAGNETIC PROPERTIES OF DYSPROSIUM METALLOCENE SMMs

3.1. Dynamic Magnetic Susceptibility Measurements and Magneto-Structural Correlations

An essential component of the magnetic property analysis was to establish the role of the cyclopentadienyl ligands and how they influence the energies of the eight Kramers doublets arising from the J = 15/2 ground term. Here, *ab-initio* theoretical studies were invaluable in

demonstrating that the magnetic ground state of Dy^{3+} in compounds of the type $[Cp_2Ln(\mu\text{-}X)]_n$ is typically a Kramers doublet with significant $M_J = \pm 15/2$ character; the main magnetic axis in this ground doublet is oriented towards the two cyclopentadienyl ligands in every case studied.[19,24-33] Hence, an axial direction can be defined according to Scheme 1, with the dominant crystal field being provided by the cyclopentadienyl ligands (see also Figures 1 and 2). The equatorial coordination sites comprises the ligands X, whose presence diminish the axiality, meaning that the SMM properties vary to an extent that depends on the μ-bridging ligand. The results of our studies are consistent with those reported by others on related metallocene SMMs, notably Long, Nippe, and Gao and Wang.[34-36]

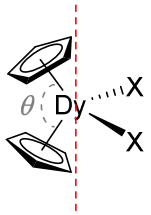

Scheme 1. The easy-axis of magnetization in the ground Kramers doublet of a dysprosium metallocene SMM.

Our first foray into the world of SMMs was a detailed study on **1**, which was found to have a small energy barrier of $U_{eff} = 32(2)$ cm^{-1} in zero applied field.[19] DFT calculations of Mayer bond orders and Mulliken population analyses revealed that the equatorial nitrogen donors in the bta 1- and 3- positions engage in strong interactions with Dy^{3+}, as do the cyclopentadienyl carbon atoms. The magneto-structural correlation in Scheme 1 implies that an appreciable, equatorial crystal field arising from the harder nitrogen donors significantly limits the magnitude of U_{eff}, whilst also producing closed hysteresis loops even at 1.8 K. Similar conclusions can be drawn

about the chloride-bridged SMMs **12-14**, which show barriers of 26(1), 68(1) and 34(1) cm^{-1}, also with narrow hysteresis loops at liquid-helium temperatures.[33]

In the thiolate-bridged SMM **2**, the soft sulfur donors provided a weaker equatorial field, leading to a larger energy barrier of 133 cm^{-1}, consistent with Scheme 1 (Figure 1).[26]

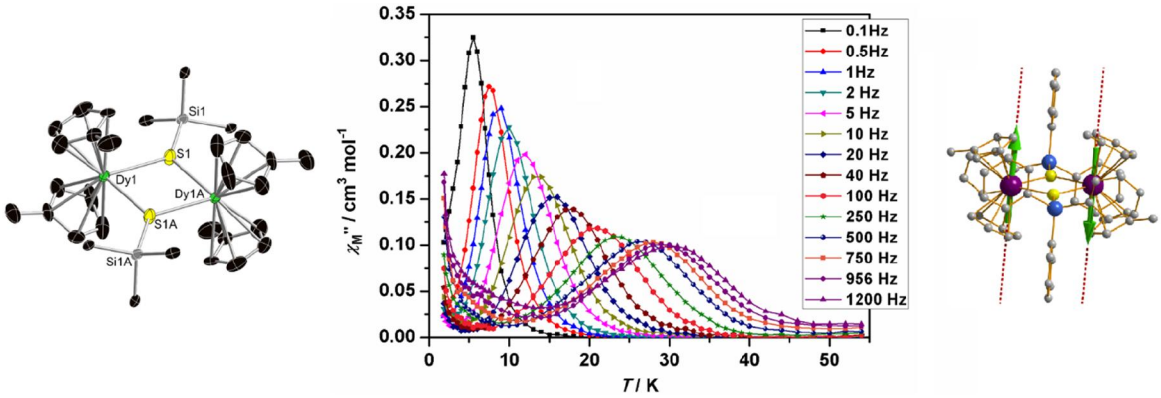

Figure 1. Molecular structure of **3** (left), and associated out-of-phase A.C. susceptibility (center) and main magnetic axes (dashed lines) of the ground Kramers doublets of Dy^{3+} (right).

A theoretical study of **1** and **3** allowed a comparison of their properties and led to a magneto-structural correlation for dysprosium metallocene SMMs. The ground Kramers doublets possess significant M_J = 15/2 character, with the easy axis of magnetization being oriented towards the methylcyclopentadienyl ligands, approximately perpendicular to the Dy···Dy axis. In the case of **3**, the calculated energy gap between the ground and first-excited doublets is 113 cm^{-1}, a sufficiently close match to the experimental energy barrier to suggest that the dominant relaxation mechanism is of the Orbach type. For **1** and **12-14**, the calculations revealed that relaxation via quantum tunneling of the magnetization (QTM) is more prominent, the main implication being that the observation of any barrier-like relaxation process is due to the axial $[Cp]^-$ ligands and the symmetry of the individual dysprosium sites, whereas the size of the

barrier is moderated by the strength of the equatorial field, i.e. softer donors should produce larger barriers than harder donor atoms.

We next turned our attention to metallocene SMMs containing phosphorus, arsenic and antimony donors. The trimetallic structures of $\mathbf{4_E}$ occur because of the steric demands of the 'flat' mesityl substituents (Figure 2).[25,27,29] Since the {Cp_2Dy} units are isostructural, these compounds provide an opportunity for studying the effects of periodic variations in the donor atom within the same p-block group. The differing degrees of non-metallic and metalloid character also potentially lead to varying covalent contributions to the metal-ligand bonds. The most obvious trend in the SMM properties of $\mathbf{4_E}$ is the gradual increase in U_{eff} on descending Group 15, i.e. U_{eff} was determined to be 210 cm^{-1}, 256 cm^{-1} and 345 cm^{-1}, respectively. The effects of exchange interactions were probed through magnetic dilution experiments; 5% or 10% dilution was achieved by synthesizing the heterobimetallic analogues [(η^5-Cp'_2Dy)(η^5-$Cp'_2Y)_2${μ-ER(H)Mes}] dispersed in a matrix of the diamagnetic species [(η^5-Cp'_2Y){μ-ER(H)Mes}]$_3$. The energy barriers in diluted $\mathbf{4_P}$ and $\mathbf{4_{As}}$ increase to 256 cm^{-1} and 301 cm^{-1}, whereas that of $\mathbf{4_{Sb}}$ remained constant. Inspection of the metric parameters in $\mathbf{4_E}$, revealed the expected significant differences in the dysprosium-pnictogen distances, i.e. 2.920(6)-2.946(6) Å, 2.984(2)-3.012(2) Å and 3.118(2)-3.195(2) Å, respectively. To rationalize the variation in U_{eff}, the diminishing influence of the formally mono-anionic equatorial ligands as the Dy–E bond length increases can be applied. A similar argument explains why the U_{eff} of 23 cm^{-1} for the arsinidene-bridged trimer $\mathbf{5_{As}}$ is larger than that of 13 cm^{-1} for phosphinidene- bridged $\mathbf{5_P}$.[25,27] Furthermore, the dramatic decrease in U_{eff} when the formal charge on the bridging ligand increases from [μ-E(H)Mes]$^-$ in $\mathbf{4_E}$ to [μ-EMes]$^{2-}$ in $\mathbf{5_E}$ can

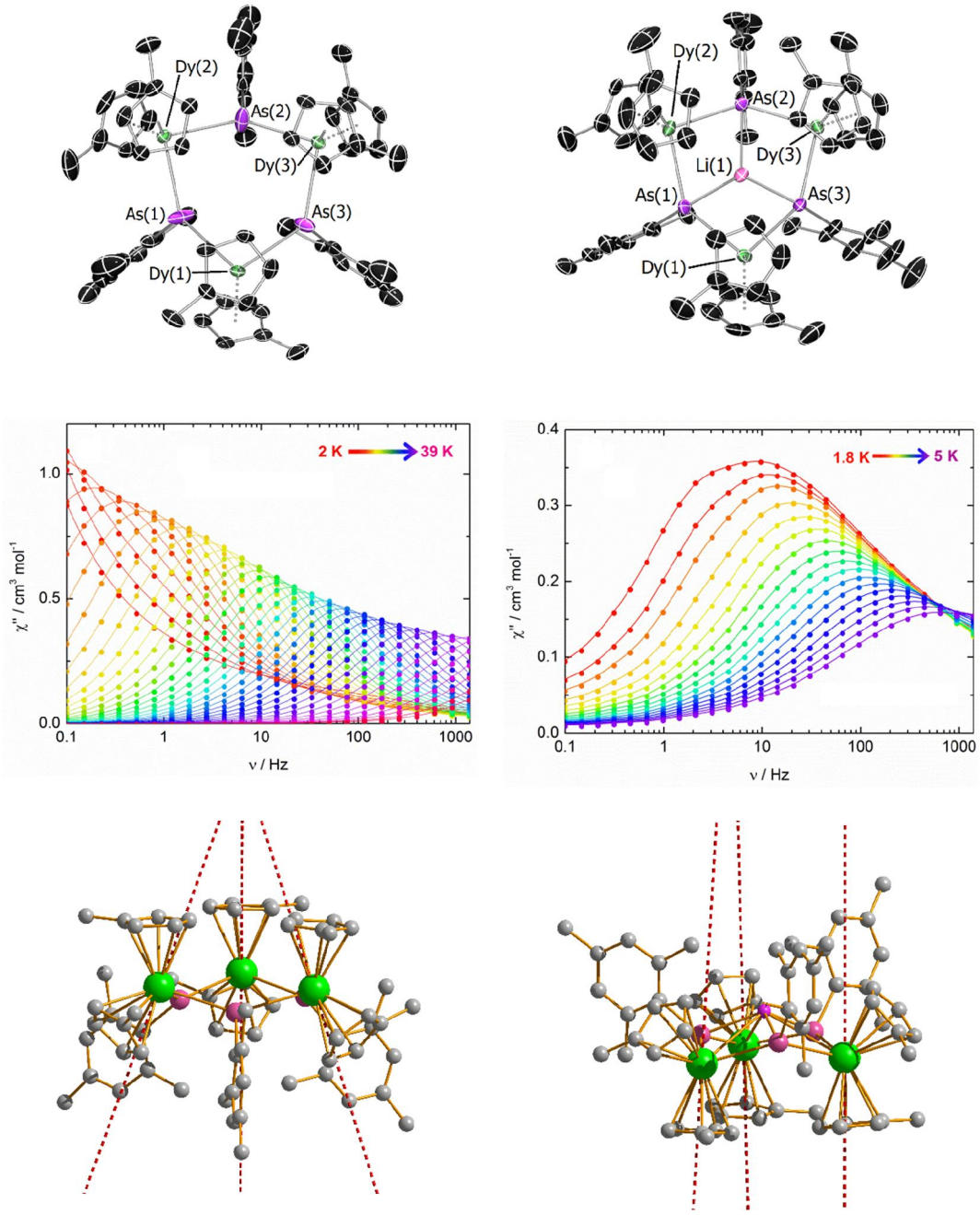

Figure 2. Molecular structure of $\mathbf{4}_{\mathbf{As}}$ and $\mathbf{5}_{\mathbf{As}}$ (top) and associated out-of-phase A.C. susceptibility (middle) and main magnetic axes (dashed lines) of the ground Kramers doublets of the Dy^{3+} ions (bottom).

also be explained by applying the magneto-structural correlation in Scheme 1, whereby the easy axis of magnetization is oriented towards the $[Cp]^-$ ligands, with the pnictogen ligands occupying the equatorial plane. Although the calculated (LoProp) charges on the bridging donor atoms were found to be much lower than the formal charges, the difference in the charge is still significant, i.e. much greater in $\mathbf{5_E}$ than in $\mathbf{4_E}$. Because the Dy–E bond lengths in $\mathbf{5_E}$ are significantly shorter than those in $\mathbf{4_E}$, the influence of the equatorial crystal field in the former is much stronger and the overall axiality of the system is diminished, along with the SMM properties.

For the selenolate-bridged trimer **2**, the U_{eff} of 252 cm^{-1} is essentially the same as in arsenide-bridged $\mathbf{4_{As}}$.[25] In terms of molecular structure, the only noteworthy difference between the two compounds is the markedly shorter Dy–E bonds in **2**, i.e. 2.9083(15)-2.9330(17) Å, however they also show similar splitting of the eight lowest-lying Kramers doublets, and so their SMM properties are closely matched. Similarly, the geometric parameters within the Zintl-ligated SMM **7** and those in $\mathbf{4_{Sb}}$ are the same within statistical error, as are the calculated energies of the lowest-lying Kramers doublets. The different U_{eff} values of $\mathbf{4_{Sb}}$ and **7**, i.e. 345 cm^{-1} and 272 cm^{-1}, respectively, are therefore likely to be linked to the charges on the equatorial antimony donor atoms. The calculated (LoProp) charges are –0.17 to –0.23 for $\mathbf{4_{Sb}}$ and –0.28 to –0.29 for **7**, with the slightly greater charges in **7** producing a smaller U_{eff}.

The observations on **1**-**7** were critical for developing a understanding of the relationship between the molecular structure and the SMM properties, particularly U_{eff} but also the blocking temperature (see below). Evidently, the observation of any slow magnetic relaxation in zero applied magnetic field is due to the strongly axial crystal field provided by the cyclopentadienyl ligands, with the equatorial heteroatom ligands moderating the magnitude of U_{eff}. In some cases, the competing equatorial field is strong enough to preclude slow relaxation in zero field, as in **6**

and **8**, where the butyl and ferrocenyl ligands promote strong mixing of the M_J states even in the ground Kramers doublet.[30] On the other hand, a very weak-field ligand would allow this hypothesis to be tested, and the charge neutral isocarbonyl ligand was identified as candidate for raising the barrier further. Not only did **11** show an extremely high energy barrier of 662 cm^{-1} in zero D.C. field, a theoretical study revealed that the dominant relaxation pathway was, unprecedentedly, via the fifth or sixth Kramers doublets, with the four lowest-lying Kramers

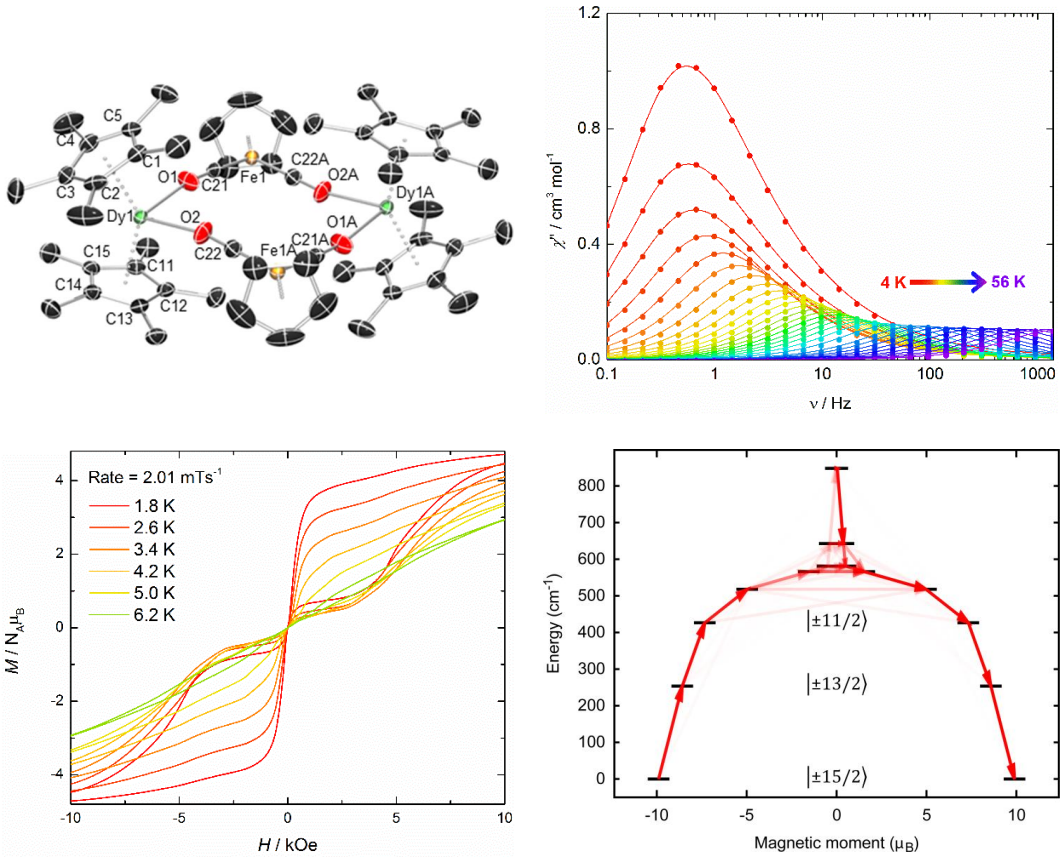

Figure 3. Molecular structure of **11** (top left) and associated out-of-phase A.C. susceptibility (top right), magnetic hysteresis (bottom left) and main magnetic axes (dashed lines) and calculated magnetic relaxation barrier (bottom right).

doublets being well described by near-pure $|M_J|$ = 15/2, 13/2, 11/2 and 9/2 states.[32] The U_{eff} value for **11** was determined by fitting the relaxation time (τ) data across the full temperature range according to equation (1).[16]

$$\tau^{-1} = \tau_0^{-1} e^{-\frac{U_{\text{eff}}}{k_B T}} + CT^n + \tau_{QTM}^{-1} \qquad (1)$$

The Orbach parameters are denoted by τ_0^{-1} and U_{eff}, the Raman parameters are denoted by C and n, and the QTM rate is τ_{QTM}^{-1}. Since typical values of the Raman exponent are n = 5-9, the best-fit value of n = 3.33 was intriguing, however such values are seemingly common in dysprosium metallocene SMMs, including a value as low as n = 2.73 for **2**.[27] The dramatic decrease in the rate of QTM upon magnetic dilution of **11** is also noteworthy, with τ_{QTM} increasing from 0.23(2) s to 17(3) s, indicating that oscillating dipolar fields on nearest-neighbour Dy^{3+} ions induce rapid relaxation.

3.2. Magnetic Hysteresis and Coercivity

Whilst the energy barriers of Ln-SMMs provide a benchmark when a new record is established, the true test lies within the magnetic hysteresis. To stand any chance of being incorporated into an 'information storage' device, molecular magnets must present a viable alternative to traditional atom-based materials currently used for this purpose, such as NdFeB magnets.[37] SMMs should be able to compete in terms of the temperatures at which they function, and in terms of coercive fields and remanent magnetization. To that end, SMMs currently offer potential, albeit some way from fulfilment. In most Ln-SMMs, the isothermal $M(H)$ hysteresis loops are S-shaped and essentially closed even at 2 K, although the effects of magnetic dilution

can open the loops at $|H| > 0$, as exemplified in Figure 3 for **11**. A sharp drop in magnetization on approaching zero field has become a hallmark of Ln-SMMs, and is taken as an indication of rapid QTM in the ground state.

Whilst many successful strategies for increasing U_{eff} have been reported, occasionally resulting in barriers >1000 cm^{-1},[38] remarkably little progress has been made towards increasing the blocking temperature beyond a few Kelvin.[9-11,13] Using the unusual $S = ½$ radical bridging ligand $[N_2]^{3-}$ in $[K(18\text{-crown-6})(thf)_2][\{(Me_3Si)_2N\}_2(thf)Tb(\mu{:}\eta^2\text{-}N_2)]$ introduces ligand-based spin density that strongly exchange couples to the 4f electrons.[39] The resulting exchange bias significantly reduces the rate of zero-field QTM, with the resulting $M(H)$ data showing a substantial coercive field of 5 T below 11 K, and with the hysteresis loops remaining open up to 14 K (sweep rate of 0.9 mT s^{-1}). Extending this strategy to $[K(2.2.2\text{-crypt})(thf)][(C_5Me_4H)_2Ln(thf)_2(\mu{:}\eta^2\text{-}N_2)]$ produced an SMM with a 100 s blocking temperature of 20 K and a giant coercive field of 7.9 T at 10 K, (sweep

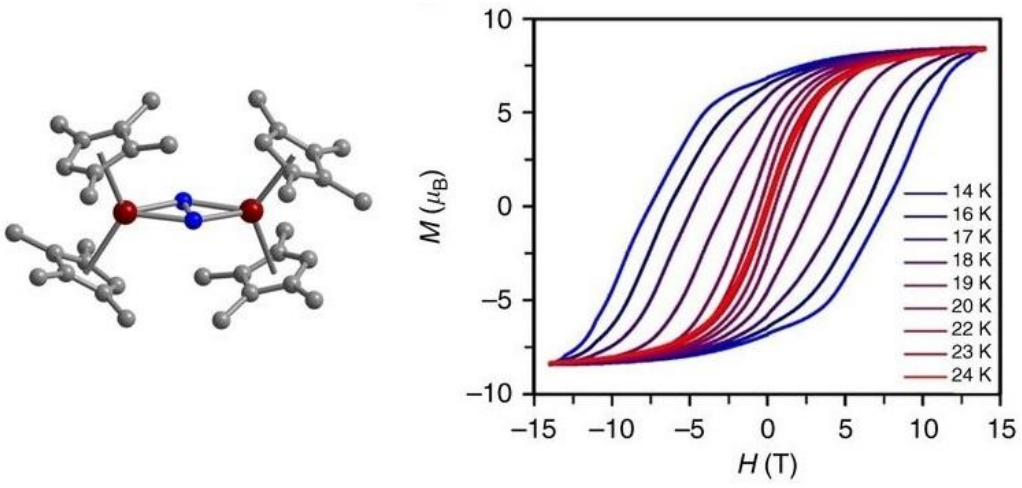

Figure 4. Molecular structure of $[(C_5Me_4H)_2Tb(thf)_2(\mu{:}\eta^2\text{-}N_2)]^-$ and the $M(H)$ hysteresis data (sweep rate of 0.01 T s^{-1}).

rate of 0.01 T s^{-1}) (Figure 4).[40] Whilst the key temperatures for these radical-bridged SMMs are still firmly in the liquid-helium regime, it has been noted that their coercive fields far exceed those of commercial rare-earth magnets, further highlighting the potential of SMMs.

Although radical-bridging ligands can have dramatic effects on the hysteresis, the site symmetry of the individual Tb^{3+} ions also plays a role in governing the magnetic anisotropy. This observation is consistent with the properties of the dimetallic SMMs **9** and **10**, in which the dysprosium ions are bridged by the dianionic, diamagnetic form and the trianionic, $S = ½$ form of the *N*,*O*-donor ligand indigo, i.e. $[ind]^{n-}$ with $n = 2, 3$, respectively. Whereas **9** and **10** are SMMs with barriers of only 39 cm^{-1} and 35 cm^{-1}, respectively, their hysteresis properties are lacking in coercivity even at 1.8 K (Figure 5). Evidently, the very low symmetry of the individual coordination sites, coupled with the strong equatorial field provided by the hard *O*- and *N*-donor atoms, is sufficient to enable rapid QTM.[31]

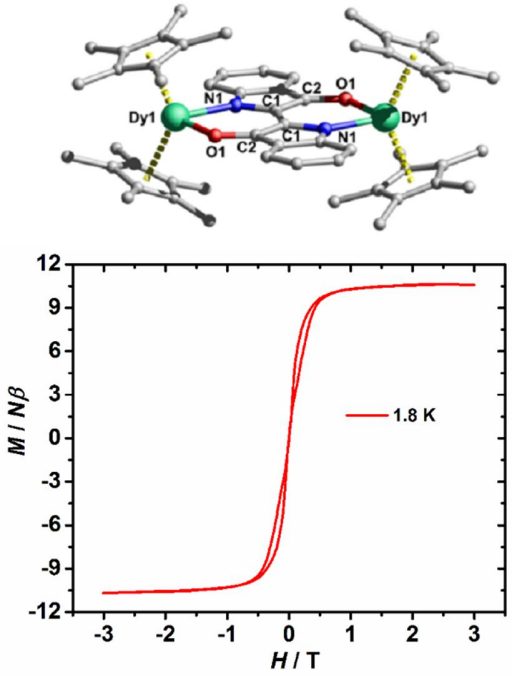

Figure 5. Molecular structure of **10** and the *M*(*H*) hyseresis data (sweep rate of 2.1 mT s^{-1}).

Having established that two cyclopentadienyl ligands provide Dy^{3+} with a strongly axial coordination environment, and that equatorial ligands limit U_{eff} whilst being highly detrimental to the hysteresis, the next logical step was to propose $[Cp_2Dy]^+$ itself as an SMM.[32] At the same time, Gao, Wang and co-workers reported *ab-initio* calculations on the hypothetical cation $[Cp^*_2Dy]^+$, which predicted exceptional magnetic axiality and an energy barrier of >1000 cm^{-1}.[36] Thus, the synthesis of $[(Cp^{ttt})_2Dy]^+[B(C_6F_5)_4]^-$ (**15**) was accomplished by reacting $[(Cp^{ttt})_2DyCl]$ with the super-electrophile $[(Et_3Si)_2H][B(C_6F_5)_4]$, the bulky ligand 1,2,4-tri(tert-butyl)cyclopentadienyl (Cp^{ttt}) preventing formation of a contact ion pair. The structural changes upon abstraction of chloride are significant, particularly the reduction in the $Dy–Cp_{cent}$ distances from 2.4126(16) Å in $[(Cp^{ttt})_2DyCl]$ to 2.32380(8) Å and 2.30923(8) Å in **15**, and the increase in the Cp-Dy-Cp angle from 147.59(7)° to 152.845(2)°.[41] These changes imply an increase in the strength of the axial crystal field, complete elimination of the equatorial field, and stronger axiality owing to the wider angle subtended at dysprosium in **15**.

In agreement with Scheme 1, $[(Cp^{ttt})_2DyCl]$ showed no clear maxima in the $\chi''(\nu)$ plots, and only very narrow hysteresis loops even at 1.8 K. In stark contrast, the $\chi''(\nu)$ data for **15** showed well-defined maxima up to 111 K, a significantly higher temperature than observed with any previously reported SMM (Figure 6). The resulting analysis yielded a new record energy barrier of 1,277 cm^{-1}. The most striking observations on **15** relate to the blocking temperature, which was determined to be 60 K from three separate experiments, i.e. the 100-second blocking temperature, the maximum temperature at which open $M(H)$ hysteresis loops were observed (average scan rate of 3.9 mT s^{-1}), and the temperature at which the FC-ZFC magnetic susceptibilities diverge (cooling rate of 2 K min^{-1}). The coercive field of 0.06 T at 60 K is also significant. These observations are consistent with the parameters reported for the same system

in a separate, independent study.[42] *Ab initio* calculations confirmed that the principal axis of magnetization in the ground Kramers doublet in **15** is oriented towards the $[Cp^{ttt}]^-$ ligands and, remarkably, that the angles formed between this axis and those of the higher doublets are less than ~5.6°. Each of the eight Kramers doublets within the $^6H_{15/2}$ multiplet is well-described by a single M_J value, with no significant mixing even in the higher-lying doublets.

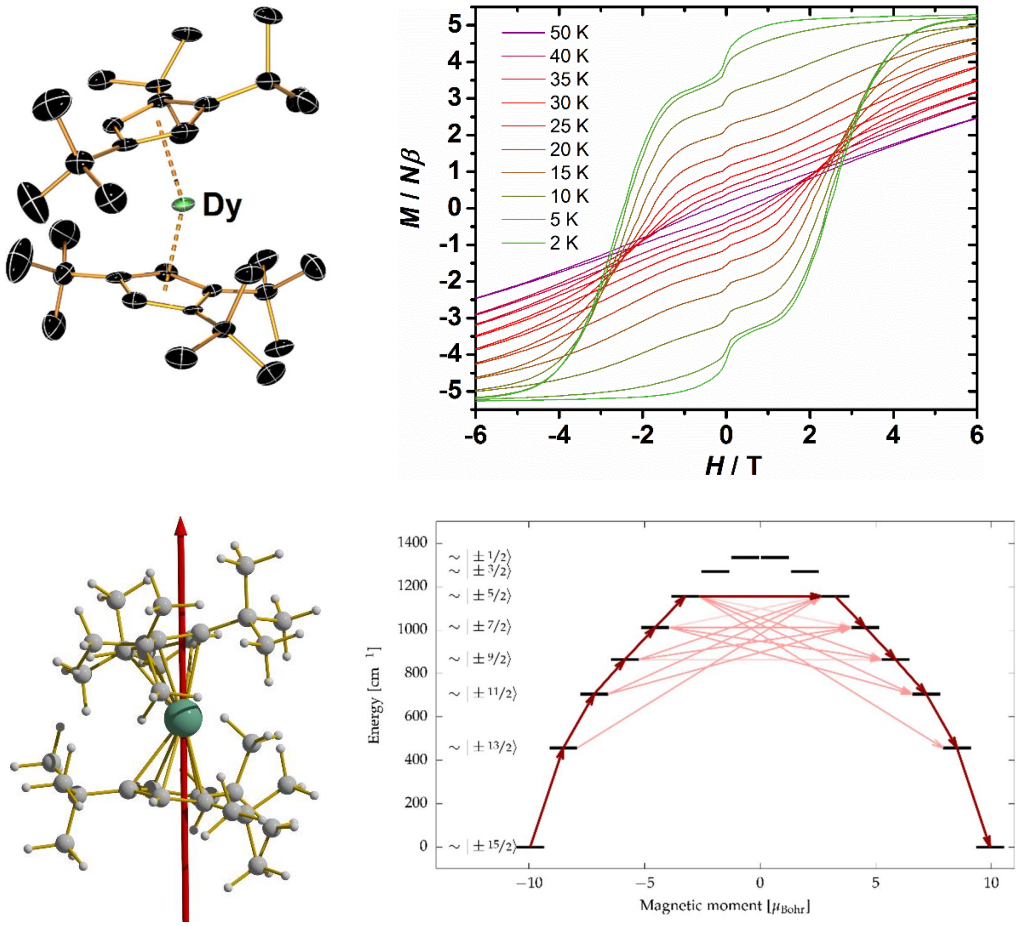

Figure 6. Molecular structure of **15** (top left), associated $M(H)$ hysteresis (top right – the loops remain open up to 60 K), main magnetic axes in the ground Kramers doublet (bottom left) and calculated magnetic relaxation barrier (bottom right).

Thus, the electronic structure of **15** is the nearest that any molecular lanthanide complex comes to being perfectly axial and, hence, U_{eff} and T_B are unprecedentedly high.

In recognising the exceptional properties of **15**, it is important to state that the most probable relaxation pathway still does not involve the highest-lying Kramers doublet despite the near-perfect axiality. More careful consideration of the electronic structure is required to explain the observed properties. Firstly, "near-perfect" is not the same as perfect, and our studies revealed that the transverse components of the *g*-tensors for each Kramers doublet are non-negligible, with the transition matrix elements connecting consecutive doublets increasing approximately by an order of magnitude. The strong QTM calculated for **15** in the sixth doublet precludes relaxation via a higher energy barrier. Consequently, our explanation of the properties incorporates a strong focus on the coordination geometry and symmetry. In a recent review, Gaita-Ariño, Coronado *et al*. asserted that such an explanation could be regarded as naïve, since the bent coordination geometry deviates significantly from an ideal uniaxial symmetry.[10d] Rather, the preferred interpretation is to invoke a dominant role for lattice vibrations and detrimental relaxation arising from spin-phonon coupling via four C–H oscillations, as proposed in a separate study on **15**.[40] However, whilst dysprosium metallocene cations remain represented by a sole example, it may be that a general explanation for the magnetic relaxation should wait until more data on closely related systems is available. More research is needed; in the meantime, the importance of structural factors such as the Cp-Dy-Cp bending angle and the steric properties of the ligand should not be overlooked.

4. OUTLOOK: TO LIQUID NITROGEN TEMPERATURES, AND BEYOND?

The properties of **15** suggest that magnetic blocking in a molecular system above the symbolic temperature of 77 K – at which nitrogen liquefies – should no longer be regarded as an insurmountable challenge. Since progress in studies of SMMs is generally experiment-led, synthetic coordination chemistry will continue to play a vital role in advancing our understanding of these fascinating materials. Ligand design is therefore critical,[43] and although varying simple properties, such as the substituents, will account for some progress, there is a strong argument for devising original chemistry. Here, one can imagine multi-decker cyclopentadienyl-dysprosium sandwich complexes possessing interesting properties, in addition to ligands rarely used in lanthanide chemistry, such as cyclobutadienyl and cyclononatetraenyl. Here, we contend that simple magneto-structural correlations, such as that proposed in Scheme 1, have a role to play.

Aside from the key performance parameters of SMMs, one must also eventually return to the issue of device technology and the possible role of organometallic compounds. The air-sensitive nature of rare-earth organometallics and their lack of thermodynamic stability are obvious technical issues that will need to be addressed before any prototype can be developed. However, if the right system can be identified, the methods of nanoscale science may adapt to incorporate such materials, and SMM-based technology may not seem so remote after all.

AUTHOR INFORMATION

Biographical Information

Dr Benjamin M. Day graduated with a Masters degree and a PhD from the University of Sussex. He has been a postdoctoral researcher in the Layfield group since 2012, studying the magnetic properties of lanthanide SMMs.

Dr Fu-Sheng Guo obtained his PhD in molecular magnetism from Sun-Yat Sen University. He was then awarded a Marie Curie International Fellowship in the Layfield group, where he works on organometallic molecular magnets.

Prof. Richard A. Layfield was appointed as Professor of Chemistry at Sussex in 2018. His research focuses on the chemistry and magnetic properties of f-block sandwich complexes and low-coordinate transition metal organometallics.

Corresponding Author

R.Layfield@sussex.ac.uk

ORCID: 0000-0002-6020-0309

Author Contributions

The manuscript was written through contributions of all authors. All authors have given approval to the final version of the manuscript.

Notes

The authors declare no competing financial interest.

ACKNOWLEDGMENT

Many of the results discussed herein would not have been possible without the pioneering synthetic methodologies developed by Dr Thomas Pugh. For generous financial support, we thank the EPSRC, the Royal Society and the European Union, including the ERC. We also thank our collaborators for their invaluable contributions; their names are listed in the references.

REFERENCES

1. Edelmann, F. T. Lanthanide and Actinides: Annual Survey of their Organometallic Chemistry Covering the Year 2017. *Coord. Chem. Rev*. **2018**, *370*, 129-223.

2. Birmingham, J. M.; Wilkinson, G. The Cyclopentadienides of Scandium, Yttrium and Some Rare Earth Elements. *J. Am. Chem. Soc.* **1956**, *78*, 42-44.

3. Watson, P. L. Methane Exchange Reactions of Lanthanide and Early-Transition-Metal Methyl Complexes. *J. Am. Chem. Soc.* **1983**, *105*, 6491-6493.

4. Nishiura, M.; Guo, F.; Hou. Z. Half-Sandwich Rare-Earth-Catalyzed Olefin Polymerization, Carbometalation, and Hydroarylation. *Acc. Chem. Res*. **2015**, *48*, 2209-2220.

5. Evans, W. J. The Expansion of Divalent Organolanthanide Reduction Chemistry Via New Molecular Divalent Complexes and Sterically Induced Reduction Reactivity of Trivalent Complexes. *J. Organomet. Chem.* **2002**, *647*, 2-11.

6. Hitchcock, P. B.; Lappert, M. F.; Maron, L.; Protchenko, A. V. *Angew. Chem. Int. Ed*. **2008**, *47*, 1488-1491.

7. (a) MacDonald, M. R.; Ziller, J. W.; Evans, W. J. *J. Am. Chem. Soc.* **2011**, *133*, 15914-15917. (b) MacDonald, M. R.; Bates, J. E.; Fieser, M. E.; Ziller, J. W.; Furche, F.; Evans, W. J. *J. Am. Chem. Soc.* **2012**, *134*, 8420-8423. (c) MacDonald, M. R.; Bates, J. E.; Ziller, J. W.; Furche, F.; Evans, W. J. *J. Am. Chem. Soc.* **2013**, *135*, 9857-9868.

8. Evans, W. J. Tutorial on the Role of Cyclopentadienyl Ligands in the Discovery of Molecular Complexes of the Rare-Earth and Actinide Metals in New Oxidation States. *Organometallics* **2016**, *35*, 3088-3100.

9. Benelli, C.; Gatteschi, D. *Introduction to Molecular Magnetism. From Transition Metals to Lanthanides*; Wiley-VCH: Weinheim, 2015.

10. (a) Gupta, S. K.; Murugavel, R. Enriching lanthanide single-ion magnetism through symmetry and axiality *Chem. Commun*. **2018**, *54*, 3685-3696. (b) Lu, J.; Guo, M.; Tang, J. *Chem. Asian J*. **2017**, *12*, 2772-2779. (c) Liu, J.-L.; Chen, Y.-C. Tong, M.-L. Symmetry strategies for high performance lanthanide-based single-molecule magnets. *Chem. Soc. Rev*. **2018**, *7*, 2431-2453. (d) Escalera-Moreno, L.; Baldoví, J. J.; Gaita-Ariño, A.; Coronado, E. Spin states, vibrations and spin relaxation in molecular nanomagnets and spin qubits: a critical perspective. *Chem. Sci*. **2018**, *9*, 3265-3275.

11. Bagai, R.; Christou, G. The *Drosophila* of Single-Molecule Magnetism: $[Mn_{12}O_{12}(O_2CR)_{16}(H_2O)_4]$. *Chem. Soc. Rev.* **2009**, *38*, 1011-1026.

12. Ishikawa, N.; Sugita, M.; Ishikawa, T.; Koshihara, S.; Kaizu, Y. Lanthanide Double-Decker Complexes Functioning as Magnets at the Single-Molecular Level. *J. Am. Chem. Soc.* **2003**, *125*, 8694-8695.

13. Woodruff, D. N.; Winpenny, R. E. P.; Layfield, R. A. Lanthanide Single-Molecule Magnets. *Chem. Rev*. **2013**, *113*, 5110-5148.

14. Leuenberger, M. N.; Loss, D. Quantum computing in molecular magnets. *Nature* **2001**, *410*, 789-793.

15. Sanvito, S. Molecular Spintronics. *Chem. Soc. Rev*. **2011**, *40*, 3336-3355.

16. Guo, Y.-N.; Xu, G.-F.; Guo, Y.; Tang, J. Relaxation dynamics of dysprosium(III) single molecule magnets. *Dalton Trans*. **2011**, *40*, 9953-9963.

17. Lin, P.-H.; Burchell, T. J.; Clerac, R.; Murugesu, M. Dinuclear dysprosium(III) single-molecule magnets with a large anisotropic barrier. *Angew. Chem. Int. Ed*. **2008**, *47*, 8848-8851.

18. Cambridge Structural Database, Conquest version 1.21, Copyright Cambridge Crystallographic Data Centre, 2018.

19. Layfield R. A.; Bashall, A.; McPartlin, M.; Rawson, J. R.; Wright, D. S. A structural and magnetic study of organolanthanide(III) amides. *Dalton Trans*. **2006**, 1660-1666.

20. Rinehart, J. R; Long, J. R. Exploiting single-ion anisotropy in the design of f-element single-molecule magnets. *Chem Sci*. **2011**, *2*, 2078-2085.

21. Ungur, L.; Chibotaru, L. F. Strategies towards high-temperature single-molecule magnets. *Inorg. Chem*. **2016**, *55*, 10043-10056.

22. (a) Ungur, L.; Le Roy, J. J.; Korobkov, I.; Murugesu, M.; Chibotaru, L.F. Fine-tuning the Local Symmetry to Attain Record Blocking Temperature and Magnetic Remanence in a

Single-Ion Magnet. *Angew. Chem. Int. Ed*. **2014**, *53*, 4413-4417. (b) Le Roy, J. J.; Ungur, L.; Korobkov, I.; Chibotaru, L.F.; Murugesu, M. Coupling Strategies to Enhance Single-Molecule Magnet Properties of Erbium-Cyclooctatetraenyl Complexes. *J. Am. Chem. Soc*. **2014**, *136*, 8003-8010. (c) Meihaus, K. R.; Long, J. R. Magnetic Blocking at 10 K and a Dipolar-Mediated Avalanche in Salts of the Bis(η^8-cyclooctatetraenide) Complex $[Er(COT)_2]-$. *J. Am. Chem. Soc*. **2013**, *135*, 17592-17597.

23. Klein, M. J. On a Degeneracy Theory of Kramers. *Am. J. Phys*. **1952**, *20*, 65-71.

24. Layfield, R. A.; McDouall, J. J. W.; Sulway, S. A.; Tuna, F.; Collison, D.; Winpenny, R. E. P. Influence of the N-Bridging Ligand on Magnetic Relaxation in an Organometallic Dysprosium Single-Molecule Magnet. *Chem.–Eur. J*. **2010**, *16*, 4442-4446.

25. Pugh, T.; Vieru, V.; Chibotaru, L. F.; Layfield, R. A. Magneto-Structural Correlations in Arsenic- and Selenium-Ligated Dysprosium Single-Molecule Magnets. *Chem. Sci*. **2016**, *7*, 2128-2138.

26. Tuna, F.; Smith, C. A.; Bodensteiner, M.; Ungur, L.; Chibotaru, L. F.; McInnes, E. J. L.; Winpenny, R. E. P.; Collison, D.; Layfield, R. A. A High Anisotropy Barrier in a Sulfur-Bridged Organodysprosium Single-Molecule Magnet. *Angew. Chem. Int. Ed*. **2012**, *51*, 6976-6980.

27. Pugh, T.; Tuna, F.; Ungur, L.; Collison, D.; McInnes, E. J. L.; Chibotaru, L. F.; Layfield, R. A. Influencing the Properties of Dysprosium Single-Molecule Magnets with Phosphorus Donor Ligands. *Nat. Commun*. **2015**, *6*, 7492.

28. Pugh, T.; Kerridge, A.; Layfield, R. A. Yttrium Complexes of Arsine, Arsenide and Arsinidene Ligands. *Angew. Chem. Int. Ed*. **2015**, *54*, 4255-4258.

29. Pugh, T.; Chilton, N. F.; Layfield, R. A. Antimony-Ligated Single-Molecule Magnets as Catalysts for Stibine Dehydrocoupling, *Chem. Sci*. **2017,** *8*, 2073-2080.

30. Grindell, R.; Day, B. M.; Guo, F.-S.; Pugh, T.; Layfield, R. A. Activation of C-H bond by rare-earth metallocene-butyl complexes, *Chem. Commun*. **2017**, *53*, 9990-9993.

31. Guo, F.-S.; Layfield, R. A. Strong Direct Exchange Coupling and Single-Molecule Magnetism in Indigo-Bridged Lanthanide Dimers, *Chem. Commun*. **2017**, *53*, 3130-3133.

32. Pugh, T.; Chilton, N. F.; Layfield, R. A. A Low-Symmetry Dysprosium Metallocene Single-Molecule Magnet with a High Anisotropy Barrier. *Angew. Chem. Int. Ed*. **2016**, *55*, 11082-11085.

33. Sulway, S. A.; Layfield, R. A.; Tuna, F.; Wernsdorfer, W.; Winpenny, R. E. P. Single-molecule magnetism in cyclopentadienyl-dysprosium chlorides, *Chem. Commun*. **2012**, *48*, 1508-1510.

34. Demir, S.; Zadrozny, J. M.; Long, J. R. Large Spin-Relaxation Barriers for the Low-Symmetry Organolanthanide Complexes $[Cp^*_2Ln(BPh_4)]$ (Cp^* = pentamethylcyclopentadienyl; Ln=Tb, Dy). *Chem. Eur. J*. **2016**, *20*, 9524-9529.

35. (a) Burns, C. P.; Wilkins, B. O.; Dickie, C. M.; Latendresse, T. P.; Vernier, L.; Vignesh, K. R.; Bhuvanesh, N. S.; Nippe, M. A comparative study of magnetization dynamics in dinuclear dysprosium complexes featuring bridging chloride or trifluoromethanesulfonate

ligands. *Chem. Commun*. **2017**, *53*, 8419-8422. (b) Burns, C. P.; Yang, X.; Wofford, J. D.; Bhuvanesh, N. S.; Hall, M. B.; Nippe, M. Structure and Magnetization Dynamics of Dy−Fe and Dy−Ru Bonded Complexes. *Angew. Chem. Int. Ed*. **2018**, *57*, 8144-8148.

36. Meng, Y.-S.; Zhang, Y.-Q.; Wang, Z.-M.; Wang, B.-W. Gao, S. Weak Ligand-Field Effect from Ancillary Ligands on Enhancing Single-Ion Magnet Performance. *Chem. Eur. J*. **2016**, *22*, 12724-12731.

37. Kawai, T.; Ma, B. M.; Sankar, S. G.; Wallace, W. E. Effect of crystal alignment on the remanence of sintered NdFeB magnets. *J. Appl. Phys*. **1990**, *67*, 4610-4612.

38. (a) Gupta, S K.; Rajeshkumar, T.; Rajaraman, G.; Murugavel, R. An air-stable Dy(III) single-ion magnet with high anisotropy barrier and blocking temperature. *Chem. Sci*. **2016**, *7*, 5181-5191. (b) Chen, Y.-C.; Liu, J.-L.; Ungur, L.; Liu, J.; Li, Q.-W.; Wang, L.-F. Ni, Z.-P.; Chibotaru, L. F.. Chen, X.-M.; Tong, M.-L. Symmetry-Supported Magnetic Blocking at 20 K in Pentagonal Bipyramidal Dy(III) Single-Ion Magnets. *J. Am. Chem. Soc*. **2016**, *138*, 2829-2837.

39. Rinehart, J. D.; Fang, M.; Evans, W. J.; Long, J. R. A N_2^{3-} radical-bridged terbium complex exhibiting magnetic hysteresis at 14 K. *J. Am. Chem. Soc*. **2011**, *133*, 14236-14239.

40. Demir, S.; Gonzalez, M. I.; Darago, L. E.; Evans, W. J.; Long, J. R. Giant coercivity and magnetic blocking temperatures for N_2^{3-} radical-bridged dilanthanide complexes upon ligand dissociation. *Nat. Commun*. **2017**, *8*, 2144.

41. Guo, F.-S.; Day, B. M.; Chen, Y.-C.; Tong, M.-L.; Mansikkamäki, A.; Layfield, R. A. A Dysprosium Metallocene Single-Molecule Magnet Functioning at the Axial Limit. *Angew. Chem. Int. Ed*. **2017**, *56*, 11145-11148.

42. Goodwin, C. A. P.; Ortu, F.; Reta, D.; Chilton N. F.; Mills, D. P. Molecular Magnetic Hysteresis in Dysprosocenium at 60 K. *Nature* 2017, **548**, 439-442.

43. Kilpatrick, A. F. R.; Guo, F.-S.; Day, B. M.; Mansikkamäki, A.; Layfield, R. A.; Cloke, F. G. N. Single-Molecule Magnet Properties of a Monometallic Dysprosium Pentalene Complex. *Chem. Commun*. **2018**, *54*, 7085-7088.